Electronic structure of Sr_2RuO_4: X-ray fluorescence emission study

E. Z. Kurmaev
Institute of Metal Physics, Russian Academy of Sciences, Ural Division, 620219 Yekaterinburg GSP-170, Russia

S. Stadler and D. L. Ederer
Department of Physics, Tulane University, New Orleans, Louisiana 70118

Y. Harada and S. Shin
Synchrotron Radiation Laboratory, Institute of Solid State Physics, University of Tokyo, 3-2-1 Midori-cho, Tanashi-shi, Tokyo 188, Japan

M. M. Grush and T. A. Callcott
Department of Physics, University of Tennessee, Knoxville, Tennessee 37996

R. C. C. Perera
Lawrence Berkeley Laboratory, Berkeley, California 94720

D. A. Zatsepin and N. Ovechkina
Institute of Metal Physics, Russian Academy of Sciences, Ural Division, 620219 Yekaterinburg GSP-170, Russia

M. Kasai and Y. Tokura
JRCAT, Tsukuba 305, Japan
and Department of Applied Physics, University of Tokyo, Tokyo 113, Japan

T. Takahashi
Department of Physics, Tohoku University, Sendai 980-77, Japan

K. Chandrasekaran, R. Vijayaraghavan, and U. V. Varadaraju
MSRC, Indian Institute of Technology, Madras 600036, India
(Received 23 June 1997; revised manuscript received 16 September 1997)

The results of measurements of O $1s$ total x-ray-fluorescence yield and Ru $N_{2,3}$ and O K_α x-ray fluorescence emission spectra of Sr_2RuO_4 and $Sr_2RuO_{4.25}$ are presented. An excitation energy dependence of the O K_α x-ray emission spectra (XES) was observed in both compounds. The energy dependence of the spectra is attributed to the excitation of inequivalent O (1) in-plane and O(2) apical oxygens. The O(1) $2p$ and O(2) $2p$ density of states distribution in the valence band of Sr_2RuO_4 was found to be different in accordance with the results of band-structure calculations. O(1) $2p$ states are found to be mixed with Ru $4d(t_{2g})$ states providing the formation of π bonds. While the O K_α XES spectra are in fair agreement with band structure calculations, the theoretical two-peak distribution of Ru $N_{2,3}$ XES is found to be different with respect to the intensity ratios and widths of the peaks of Ru $N_{2,3}$ XES. These differences are attributed to a decrease of intensity of radiative $4d \rightarrow 4p$ transitions in the vicinity of the Fermi level (where the localization of Ru $4d$ states is higher than at the bottom of the valence band) due to a strong Koster-Kronig transition. [S0163-1829(98)00704-8]

I. INTRODUCTION

The electronic structure of Sr_2RuO_4 has been discussed intensively during the last few years[1–9] due to the discovery of superconductivity ($T_c = 0.93$ K)[10] in this first copperless oxide superconductor having a layered perovskite structure. This material has the same crystal structure as La_2CuO_4 with RuO_2 planes replacing the CuO_2 planes. As with the cuprates the resistivity in-plane and perpendicular to the plane is highly anisotropic. On the other hand, some differences between Sr_2RuO_4 and high-T_c superconductors (HTSC's) have been observed: (i) Sr_2RuO_4 is superconducting without any chemical doping, which is not typical for cuprates, (ii) the d orbitals involved in hybridization with oxygen $2p$ states are different; they are of the t_{2g} type (d_{xy}, d_{xz}, d_{yz}) in Sr_2RuO_4 and of the e_g type ($d_{x^2-y^2}$) in copper oxides, (iii) the density of states at the Fermi level is four times greater for Sr_2RuO_4 than for $YBa_2Cu_3O_{7-\delta}$, and (iv) Sr_2RuO_4 shows an enhanced Pauli paramagnetism while La_2CuO_4 is an antiferromagnetic insulator. These differences and similarities in the properties of Sr_2RuO_4 compared with HTSC's stimulate a deeper study of its electronic structure. In spite of several band-structure calculations of Sr_2RuO_4 (Refs. 1–3) only a few ultraviolet photoemission spectroscopy (UPS),[6] x-ray photoemission spectroscopy (XPS),[8] and angle-resolved photoemission spectroscopy (ARPES)[4,5] spectral measurements are available. The unoccupied O $2p$ states of Sr_2RuO_4 have been investigated with the help of O $1s$ NEXAFS spectroscopy[6] and some features of the O $1s$ absorption spectra were assigned to different oxygen atoms. Such infor-

mation for the valence band can be obtained with soft x-ray emission spectroscopy with tunable excitation as was shown for $La_{2-x}Sr_xCuO_4$,[11] $Bi_2Sr_2CaCu_2O_{8+\delta}$, and $Tl_2Ba_2CaCu_2O_8$.[12]

In this paper, we present the first experimental spectral study of the selectively excited Ru $N_{2,3}$ ($4d \rightarrow 4p$ transition) and O $K\alpha$ ($2p \rightarrow 1s$ transition) x-ray emission spectroscopy (XES) measurements for stoichiometric Sr_2RuO_4 and overdoped $Sr_2RuO_{4.25}$. We have shown that one can selectively excite specific oxygen sites by tuning the excitation energy because the O $1s$ absorption cross section between in-plane and apical oxygen atoms is different. In such a way, the distribution of O(1) $2p$ and O(1)+O(2) $2p$ states in the valence band is determined. Our results show that the O $K\alpha$ XES spectra are in a good agreement with band-structure calculations whereas the intensity distribution of the Ru $N_{2,3}$ XES does not coincide with the Ru $4d$ density of states distribution in the valence band of Sr_2RuO_4. These differences are attributed to decreasing of intensity of radiative $4d \rightarrow 4p$ transitions in the vicinity of the Fermi level (where the localization of Ru $4d$ states is higher than at the bottom of the valence band) due to strong Koster-Kronig transition.

II. EXPERIMENT

The spectral measurements are performed using both single-crystal and ceramic samples. The single crystal of Sr_2RuO_4 was prepared by the floating zone method as described in Ref. 4. Ceramic $Sr_2RuO_{4.25}$ was synthesized using high-purity RuO_2 and $SrCO_3$ by heating to 900 °C for 24 h followed by an additive heat treatment at 1200 °C for 48 h. Finally the sample was maintained at 900 °C for 24 hours in an oxygen flow. An oxygen flow was maintained while the furnace was cooled. A stoichiometric sample of Sr_2RuO_4 was obtained by heating $Sr_2RuO_{4.25}$ to 900 °C in an argon flow for 24 h followed by cooling in an argon flow. The lattice parameters of the samples were $a=3.868$ Å and $c=12.746$ Å for $Sr_2RuO_{4.25}$ and $a=3.876$ Å and $c=12.732$ Å for Sr_2RuO_4. Resistivity measurements in the temperature range 300 to 15 K indicate that $Sr_2RuO_{4.25}$ is semiconducting with the values ρ_0 (300 K)=30 mΩ cm and ρ_0 (15 K) =90 mΩ cm, whereas Sr_2RuO_4 is degenerate with the values of about ρ_0 (300 K) and ρ_0 (15 K) equal to 10 mΩ cm.

The measurements of O $K\alpha$ x-ray emission spectra near the O $1s$ threshold were performed at the Advanced Light Source on beamline 8.0, which is described in detail elsewhere.[13] The fluorescent radiation emitted from the sample was energy analyzed with a high-resolution grating spectrometer and a computer-interfaced multichannel detector. The pressure in the sample chamber was below 10^{-9} torr during the measurements. The resolution of the beamline monochromator was set to 0.5 eV for 530 eV photon energy. The O $K\alpha$ x-ray emission spectra were recorded using a 1500 lines/mm grating ($R=10$ m) in the first order of diffraction with the spectrometer resolution set to 0.3 eV.

The measurements of Ru $N_{2,3}$ XES at $E=200$ eV and O $1s$ total fluorescence yield (TFY) spectra were performed on a BL-19B undulator beamline[14] of the Photon Factory located at the National Laboratory for High Energy Physics (KEK). Synchrotron radiation was monochromatized by a grazing incidence monochromator. The energy resolution of monochromator was about 0.1 eV for O $1s$ TFY and 0.03 eV for Ru $N_{2,3}$ XES. The energy resolution of spectrometer was 0.1 eV for O $1s$ TFY and Ru $N_{2,3}$ XES.

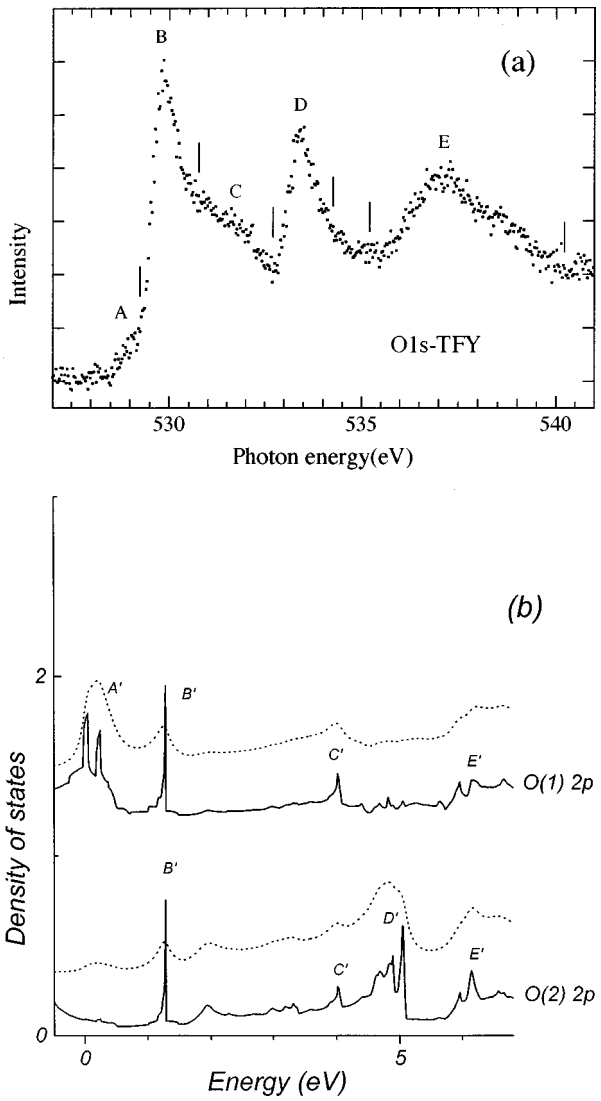

FIG. 1. (a) The x-ray absorption spectrum of Sr_2RuO_4 near the O K edge. (b) The results of band-structure calculations of the conduction band of Sr_2RuO_4 [adapted from Ref. 2 (solid line) and the O $2p$ DOS broadened for instrumental resolution $E=0.1$ eV (dotted line)].

O $K\alpha$ XES of Sr_2RuO_4, $Sr_2RuO_{4.25}$ and reference sample $EuMnO_3$ were calibrated independently using electron-beam excited spectral measurements from another grating spectrometer under experimental conditions similar to those described in Refs. 15 and 16.

III. RESULTS AND DISCUSSION

The soft x-ray absorption spectrum of Sr_2RuO_4 measured near the O K edge using total fluorescence yield (TFY) detection is given in Fig. 1(a). The results are similar to O 1s NEXAFS measurements of Sr_2RuO_4. According to band-structure calculations of Singh[2] reproduced in Fig. 1(b) one can attribute the origin of peak A at $E \sim 528.5$ eV to a transition of O $1s$ electron to O(1) $2p$ unoccupied states (A') just above the Fermi energy. From the calculations presented

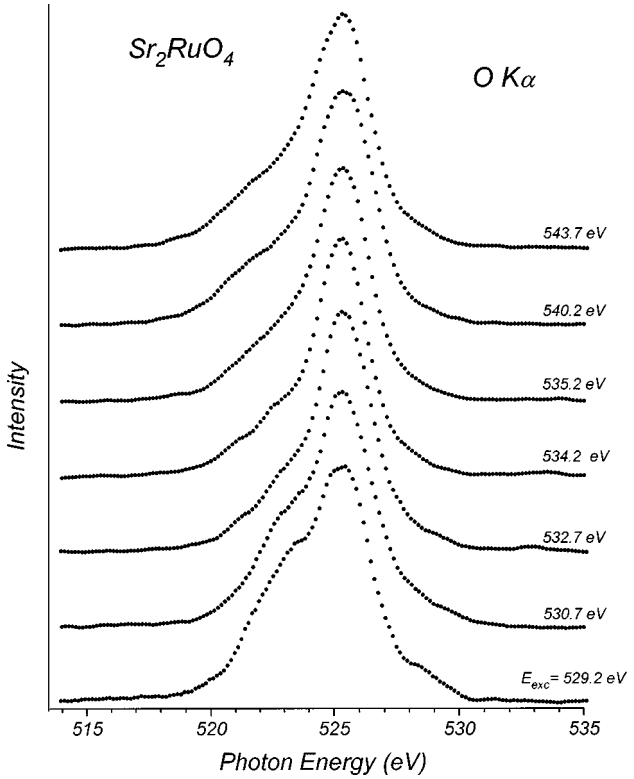

FIG. 2. The O $K\alpha$ x-ray emission spectra of Sr_2RuO_4 at different excitation energies.

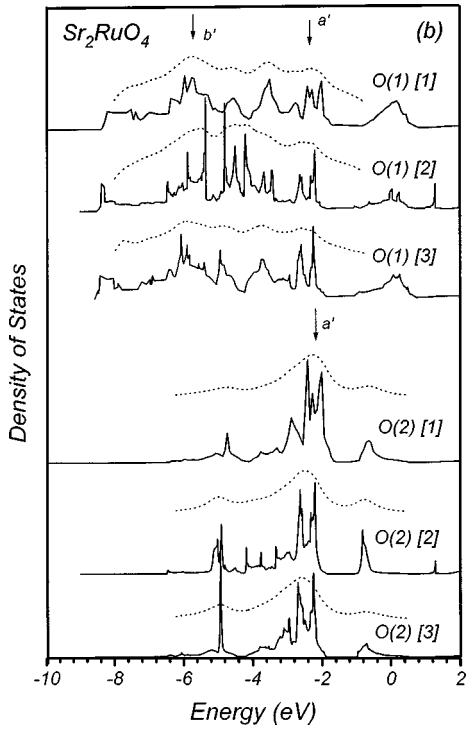

FIG. 3. O(1), O(2) $2p$ density of states distribution in the valence band of Sr_2RuO_4 taken from local-density approximation band-structure calculations of Sr_2RuO_4 of Oguchi (Ref. 1), Singh (Ref. 2), and Hase (Ref. 3). The O $2p$ DOS broadened for instrumental resolution $\Delta E = 0.3$ eV are shown by the dotted line.

in Fig. 1(b) the O(2) $2p$ density of states (DOS) contribution is very small in the region extending a few eV above the Fermi energy. We attribute feature B and C of O $1s$ TFY spectrum located at $E \sim 530$ and 531.5 eV, respectively, to a comparable mixture of O(1) and O(2) $2p$ states [B' and C' in Fig. 1(b)]. From Fig. 1(b) we observe the increasing contribution to the O(2) $2p$ state (D') and interpret the increasing fluorescence up to feature D at $E \sim 533.5$ eV in Fig. 1(a) to these states. As the excitation energy continues to increase, the O(1) $2p$ channel shows an increasing density of states at E' about 6 eV above the threshold. This increase is described as a mixing of unoccupied O(1) and O(2) $2p$ states in O $1s$ TFY spectrum between 536 and 540 eV [Fig. 1(a)].

Figure 2 shows the O $K\alpha$ XES ($2p \rightarrow 1s$ transition) of Sr_2RuO_4 recorded at selected excitation energies indicated by the vertical lines in Fig. 1(a). O $K\alpha$ x-ray emission probes the valence-band states with p symmetry. As the excitation energy increases, the peak at $E = 523$ eV is reduced to a shoulder. Increasing the excitation energy leads to a decreasing of the intensity of O $K\alpha$ XES high-energy shoulder at $E = 528 - 530$ eV. At excitation energy $E \sim 534.2$ eV, the O $K\alpha$ XES valence spectrum is a narrower and more symmetrical band. This spectrum is quite different with respect to that obtained at $E \sim 529.2$ eV and 543.7 eV, and can be taken as reference to show the dependence of the shape of the spectra on variation of excitation energy.

O $K\alpha$ XES of $Sr_2RuO_{4.25}$ measured at different excitation are very similar to those of the stoichiometric compound Sr_2RuO_4 shown in Fig. 2. As in the case of Sr_2RuO_4, we have found significant differences in the fine structure of O $K\alpha$ XES excited at $E = 529.2$ eV and $E = 533.2$ eV. Evidence of overdoped oxygen in O $K\alpha$ XES spectra of $Sr_2RuO_{4.25}$ is not detected most probably because of the small level of overdoping with respect to that of the stoichiometric compound.

The extremely high sensitivity of the O $K\alpha$ XES to excitation energy can be attributed to the significant differences between in plane [O(1)] and out of plane-apical [O(2)] $2p$ DOS in Sr_2RuO_4. According to LDA band structure calculations,[1–3] the distribution of O(1) $2p$ DOS has an extended two-peak character, while the center of gravity of O(2) $2p$ states is shifted to the top of the valence band and is much narrower (Fig. 3).

In Fig. 4 the experimental O $K\alpha$ XES of Sr_2RuO_4 excited at 529.2 and 534.2 eV are adjusted to the binding-energy scale using O $1s$ XPS binding energy data. According to XPS measurements of Sr_2RuO_4, the O $1s$ spectrum is split into two lines ($\Delta E \sim 0.8$ eV) (Ref. 8), which exposes the differences in O $1s$ binding energies (be's) of O(1) and O(2) atoms occupying non-equivalent positions. A similar difference ($\Delta E = 1.45$ eV) of O $1s$ be's for O(1) and O(2) atoms is predicted by band-structure calculations of Singh.[2] It is observed that the experimental O $K\alpha$ XES of Sr_2RuO_4 measured at $E \sim 534.2$ is similar to the calculated O(2) $2p$ DOS of Sr_2RuO_4 (Fig. 3). On the other hand, the O $K\alpha$ XES of Sr_2RuO_4 selectively excited at 529.2 eV show a splitting ($a - b$) that can be attributed to the splitting O(1) $2p$ DOS (see features of $a' - b'$ in Fig. 3). At higher excitation energies [for instance, at $E \sim 543.7$ eV (Fig. 2)] O $K\alpha$ XES of Sr_2RuO_4 can be simulated by a superposition of these spectra, which corresponds to superposition of O(1) $2p$ and O(2) $2p$ DOS.

In Fig. 5 O $K\alpha$ XES spectra of the $Eu_{0.7}Ca_{0.3}MnO_3$ per-

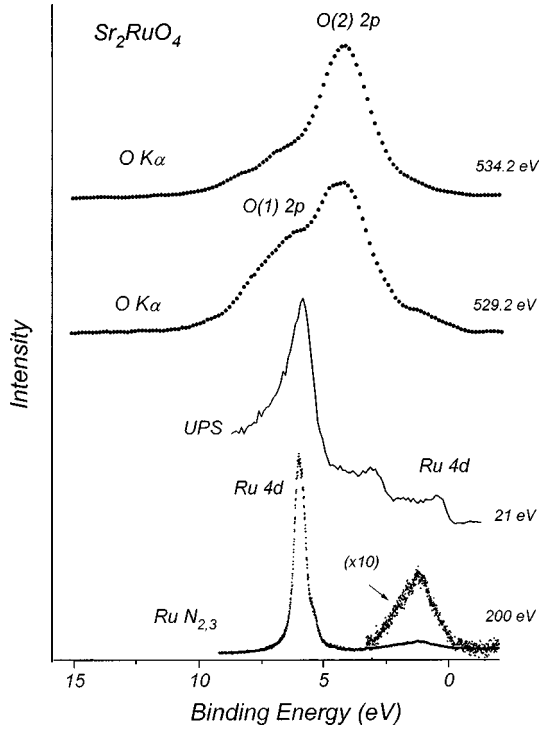

FIG. 4. The comparison of the experimental Ru $N_{2,3}$ XES (measured at $E=200$ eV), O $K\alpha$ XES (measured at $E=529.2$ and 534.2 eV) with the UPS of Sr_2RuO_4 excited at $E=21$ eV.

ovskite are shown. No excitation energy dependence was found even though the crystal structure of undoped orthorhombic $EuMnO_3$ has two inequivalent oxygen atoms: O(1) in plane and O(2) interplane. According to XPS measurements[17] the O $1s$ line is not split in $EuMnO_3$, which means that these oxygens have very close binding energies. On the other hand, the $2p$ density of states distribution is found to be similar for in-plane and interplane oxygens.[17] This supports the above given interpretation of the high sensitivity of O $K\alpha$ XES of Sr_2RuO_4 to the variation of the excitation energy near O $1s$ threshold as a result of selective excitation of O(1) and O(2) atoms.

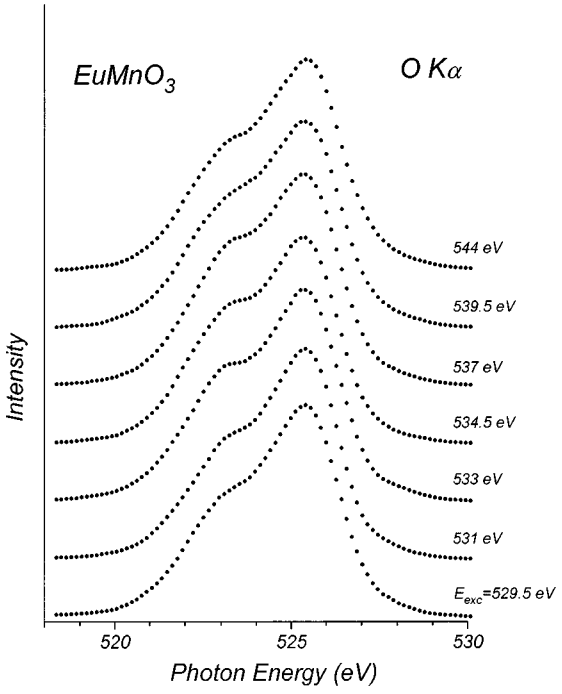

FIG. 5. The O $K\alpha$ XES of $EuMnO_3$ recorded at different excitation energies.

The comparison of Ru $N_{2,3}$, O(1) and O(2) $K\alpha$-emission bands with the UPS spectrum of Sr_2RuO_4 excited at $E=21$ eV (Ref. 8) is shown in Fig. 4 (Ru $N_{2,3}$ is converted to the binding-energy scale using XPS Ru $4p$ measurements ($E=44.7$ eV). Taking into account the values of photoionization cross sections of O $2p$ and Ru $4d$ states,[18] one can conclude that UPS spectra excited at 21 eV probe both Ru $4d$ and O $2p$ states. On the other hand, O $K\alpha$ and Ru $N_{2,3}$ XES probes O $2p$ and Ru $4d$ states directly because of the dipole selection rules ($2p\rightarrow 1s$ and $4d\rightarrow 4p$ transitions, respectively). It is necessary to point out that the energy position of the subband of O $K\alpha$ XES excited at $E=529.2$ eV coincides with the peak of the UPS spectrum located at 5.7 eV (Fig. 4). The maximum intensity of O $K\alpha$ XES excited at 534.2 eV does not coincide completely with the UPS peak located at 2.6 eV. This means that O $K\alpha$ XES excited at 534.2 eV has a high weight of O(2) $2p$ states, but still has some contribution of O(1) $2p$ states.

The most intensive peak of Ru $N_{2,3}$ XES located at 6 eV is very close to the subband of O $K\alpha$ XES excited at 529.2 eV. This means that Ru $4d$ states are mostly hybridized with O(1) $2p$ states, which is in accordance with band-structure calculations.[1–3] According to angle-resolved photoemission measurements of Sr_2RuO_4,[4] these Ru $4d$ states are derived from d_{xy}, d_{xz}, and d_{yz} orbitals. Using classification, given in Ref. 19, one can conclude that O(1) $2p$ states that are mixed with Ru $4d_{xy,xz,yz}$ states form π bonds, fully accord with the results of LDA band-structure calculations.[1–3] These differences in electronic structure of Sr_2RuO_4 and superconducting cuprates, where Cu $3d_{x^2-y^2}$–O $2p\sigma$ hybridization is found,[20] can be due to a different number of electrons in Ru and Cu. In the case of the cuprates, the $d_{x^2-y^2}$ and d_{z^2} orbitals (the σ orbitals) are responsible for bonding, while in the case of Sr_2RuO_4 these two σ orbitals are entirely empty with $d_{xy,xz,yz}$ orbitals (π orbitals) being responsible for bonding.

It is seen from Fig. 4 that Ru $N_{2,3}$ XES is split into two subbands located at 1.2 and 6 eV. A similar two-peak distribution of Ru $4d$ DOS is found in band-structure calculations,[1–3] hovewer, with opposite peak ratio: Ru $4d$ density of states at the vicinity of the Fermi level is 2–2.5 times greater than that of the bottom of the valence band. The theoretical distribution of the Ru $4d$ states at the bottom of the valence band is found to be more extended than the width of the peak of Ru $N_{2,3}$ XES located at 6 eV. The differences in intensity ratios and widths of the peaks between experimental (Fig. 4) and theoretical Ru $4d$ DOS (Refs. 1–3) can be attributed to the interaction of a core-level hole with a valence-band hole that is stronger for Ru $N_{2,3}$ XES than for O $K\alpha$ XES because of strong overlapping of Ru $4p$ and Ru $4d$ wave functions. For this reason a strong super Koster-Kronig transition takes place and a nonradiative decay process is more probable than a radiative one. Therefore, this interaction can distort the Ru $4d$ density of states distribution in the valence band obtained from Ru $N_{2,3}$ XES. According to band-structure calculations,[1–3] the localization

of Ru $4d$ states in the vicinity of the Fermi level is higher than at the bottom of the valence band, where they are hybridized with O(1) $2p$ states. This means that the super Koster-Kronig transition is stronger for Ru $4d$ states located close to the Fermi level, which can be responsible for the decrease of intensity of radiative transitions in this region.

IV. CONCLUSION

In summary, we present an experimental spectral study of the electronic structure of Sr_2RuO_4 and $Sr_2RuO_{4.25}$ using x-ray emission spectroscopy. An excitation energy dependence of O $K\alpha$ x-ray emission spectra was observed in both compounds. The energy dependence of the observation is attributed to the excitation of inequivalent O(1) in-plane and O(2) apical oxygens. The O(1) $2p$ and O(2) $2p$ density of states distribution in the valence band of Sr_2RuO_4 was found to be different in accordance with the results of band-structure calculations. O(1) $2p$ states are found to be mixed with Ru $4d(2_g)$-states providing the formation of π bonds. While the O $K\alpha$ XES spectra are in fair agreement with band-structure calculations, the theoretical two-peak distribution of the Ru $4d$ DOS is found to be different with respect to intensity ratios and width of the peaks of Ru $N_{2,3}$XES. These differences are attributed to a decrease of intensity of radiative $4d \rightarrow 4p$ transitions in the vicinity of the Fermi level (where the localization of Ru $4d$ states is higher than at the bottom of the valence band) due to strong Koster-Kronig transition.

ACKNOWLEDGMENTS

We are grateful to Dr. Ya. M. Mukovskii for preparing the reference sample $EuMnO_3$, Dr. D. Singh, Dr. T. Oguchi, and Dr. I. Hase for making available the full data of their band-structure calculations, and Dr. M. Matteucci for participation in measurements and discussion. This work was supported by Russian State Program on Superconductivity (Project 95026), Russian Science Foundation for Fundamental Research (Project Nos. 96-03-3209 and 96-15-96598), NATO Linkage Grant (HTECH.LG 971222), the NSF Grants Nos. DMR-901 7997 and DMR-9420425, and the DOE EPSCOR and Louisiana Education Quality Special Fund [Grant No. DOE-LEQSF (1993-95)-03]. The work at the Advanced Light Source at Lawrence Berkeley National Laboratory was supported by the U.S. Department of Energy (Contract No. DE-AC03-76SF00098).

[1] T. Oguchi, Phys. Rev. B **51**, 1385 (1995).
[2] D. J. Singh, Phys. Rev. B **52**, 1358 (1995).
[3] I. Hase and Y. Nishihara, J. Phys. Soc. Jpn. **65**, 3965 (1996).
[4] T. Yokoya, A. Chainani, T. Takahashi, H. Katayama-Yoshida, M. Kasai, and Y. Tokura, Phys. Rev. Lett. **76**, 3009 (1996); T. Yokoya, A. Chainani, T. Takahashi, H. Ding, J. C. Campuzano, H. Katayama-Yoshida, M. Kasai, and Y. Tokura, Phys. Rev. B **54**, 13 311 (1996).
[5] D. H. Lu, M. Schmidt, T. R. Cummins, S. Schuppler, F. Lichtenberg, and J. G. Bednorz, Phys. Rev. Lett. **76**, 4845 (1996).
[6] M. Schmidt, T. R. Commins, M. Burk, D. H. Lu, N. Nicker, S. Schuppler, and F. Lichtenberg, Phys. Rev. B **53**, R14 761 (1996).
[7] G. Baskaran, Physica B **223-224**, 490 (1996).
[8] T. Yokoya, A. Chainani, T. Takahashi, H. Katayama-Yoshida, M. Kasai, Y. Tokura, N. Shanthi, and D. D. Sarma, Phys. Rev. B **53**, 8151 (1996).
[9] G. J. McMullan, M. P. Ray, and R. J. Needs, Physica B **223-224**, 529 (1996).
[10] Y. Maeno, H. Hashimoto, K. Yoshida, S. Nishizaki, T. Fujita, J. C. Bednorz, and F. Lichtenberg, Nature (London) **372**, 532 (1994).
[11] J.-H. Guo, S. M. Butorin, N. Wassdahl, P. Skytt, J. Nordgren, and Y. Ma, Phys. Rev. B **49**, 1376 (1994).
[12] S. M. Butorin, J.-H. Guo, N. Wassdahl, P. Skytt, J. Nordgren, Y. Ma, C. Stræm, L.-G. Johansson, and M. Qvarford, Phys. Rev. B **51**, 11 915 (1995).
[13] J. J. Jia, T. A. Callcott, J. Yurkas, A. W. Ellis, F. J. Himpsel, M. G. Samant, J. Stæhr, D. L. Ederer, J. A. Carlisle, E. A. Hudson, L. J. Terminello, D. K. Shuh, and R. C. C. Perera, Rev. Sci. Instrum. **66**, 1394 (1995).
[14] M. Fujisawa, A. Harasawa, A. Agui, M. Watanasbe, A. Kakizaki, S. Shin, T. Ishii, T. Kita, T. Harada, Y. Saitoh, and S. Suga, Rev. Sci. Instrum. **67**, 345 (1996).
[15] V. V. Fedorenko, V. R. Galakhov, L. V. Elokhina, L. D. Finkelstein, V. E. Naish, E. Z. Kurmaev, S. M. Butorin, E. J. Nordgren, A. K. Tyagi, U. R. K. Rao, and R. M. Iyer, Physica C **221**, 71 (1994).
[16] A. V. Postnikov, St. Bartkowski, F. Mersch, M. Neumann, E. Z. Kurmaev, V. M. Cherkashenko, S. N. Nemnonov, and V. R. Galakhov, Phys. Rev. B **52**, 11 805 (1995).
[17] E. Z. Kurmaev, V. M. Cherkashenko, M. Neumann, S. Stadler, D. L. Ederer, Ya. M. Mukovskii, I. V. Solovyev, N. Ovechkina, V. R. Galakhov, A. Fujimori, M. M. Grush, T. A. Callcott, and R. C. C. Perera (unpublished).
[18] J. J. Yeh and I. Lindau, At. Data Nucl. Data Tables **32**, 1 (1985).
[19] L. F. Mattheiss, Phys. Rev. B **13**, 2433 (1976).
[20] L. F. Mattheiss and D. R. Hamann, Phys. Rev. B **40**, 2217 (1989).